Kinetics of Folding of Leucine Zipper Domains†

Hans Wendt,‡ Christine Berger,‡ Antonio Baici,§ Richard M. Thomas,|| and Hans Rudolf Bosshard*,‡

Biochemisches Institut der Universität Zürich, Winterthurerstrasse 190, CH-8057 Zürich, Switzerland, Rheumaklinik, Universitätsspital, CH-8091 Zürich, Switzerland, and Institut für Polymere, ETH-Zentrum, CH-8092 Zürich, Switzerland

Received November 11, 1994; Revised Manuscript Received December 30, 1994⊗

ABSTRACT: Leucine zippers are short coiled coils frequently found in transcription factors where they serve as dimerization domains. The basic features contributing to the thermodynamic stability of leucine zippers are well understood, but very little is known about their folding kinetics. Leucine zippers have a simple and well defined structure and are, therefore, excellent models for the study of the concerted folding and assembly of polypeptide chains. Here we report on a fluorescence stopped flow investigation of the kinetics of association and dissociation of a series of model leucine zippers based on the common sequence X_0-EYEALEKKLAAX_1EAKX_2QALEKKLEALEHG-amide (X_0 = N^{α}-acetyl, N^{α}-fluorescein-GGG, or N^{α}-dimethylaminocoumarin-GGG; X_1 = Leu or Ala; X_2 = Leu, Ala, or Asn). When X_0 is fluorescein, self-quenching between adjacent fluorophores leads to a decrease in fluorescence emission intensity whereas unfolding of the coiled coil leads to an increase. In a heteromeric coiled coil containing both fluorophores, resonance energy transfer between the donor coumarin and the acceptor fluorescein is observed, and the mixing of labeled and nonlabeled peptides allows the measurement of the rates of strand exchange between leucine zippers. Exchange rates do not depend on peptide concentration, indicating that strand exchange is governed by the rate of dissociation of the coiled coil. Strand exchange between leucine zippers with X_1 and X_2 = Leu occurs with a half-time of ≈30 min. A single Leu/Ala substitution at X_1 or X_2 decreases the half-time to ≈1 s. Folding was also studied in a relaxation experiment in which a preexisting equilibrium between monomeric chains and coiled coils was rapidly disturbed by dilution with buffer, and the relaxation to the new equilibrium was followed by the increase in fluorescence. In peptides with X_1, X_2 = Ala or X_1 = Ala, X_2 = Asn the folding process can be described by a simple two-state monomer ⇄ dimer equilibrium with $k_{on} \approx 4 \times 10^6$ M^{-1} s^{-1} and $k_{off} \approx 10$ s^{-1}. $K_d = k_{off}/k_{on} \approx 2.5$ μM is in good agreement with the value of K_d obtained from equilibrium measurements. The peptides with a single Ala at X_1 or X_2 exhibit biphasic folding kinetics. One phase is concentration dependent and the other apparently concentration independent. This behavior can be interpreted as a monomer ⇆ dimer equilibrium coupled to an equilibrium between different conformational isomers. Leu to Ala and Leu to Asn substitutions in the hydrophobic core alter the folding kinetics in a position-dependent manner. The stabilities of the model leucine zippers are similar to those of transcription factors, and their folding is a very rapid and highly concerted reaction with a half-time ≈100 ms at 1 μM peptide concentration. The rapid association and dissociation and strand exchange may be of importance to the biological function of the leucine zipper domains of transcription factors.

In their simplest form leucine zippers consist of two peptides in an approximately α-helical conformation wound around each other to form a coiled coil. The structure is based on a repeating seven-residue motif (*a b c d e f g*) in which Leu occupies the *d* position and β-branched amino acids are frequent at *a*. Leucine zippers mediate the dimerization of two arginine-rich domains to form a DNA-binding site in the basic-leucine-zipper and the basic-helix-loop-helix families of transcription factors (Harrison, 1991; Hurst, 1994), and, more generally, coiled coils serve to oligomerize protein subunits. The X-ray structure of the parallel, dimeric leucine zipper domain GCN4-p1 of the yeast transcriptional activator protein GCN4 has been solved (O'Shea et al., 1991).[1] This structure, together with numerous studies on model leucine zipper peptides (Zhu et al., 1992; Zhou et al., 1992; Graddis et al., 1993), has revealed the basic features of coiled coil domains. Alternate layers of residues at *d* and *e* and at *g* and *a* interact side-by-side with the corresponding residues of the adjacent strand to form an uninterrupted hydrophobic interface. Charged residues at *g* and *e*, at the outer layer of the hydrophobic interface, may lead to interhelical ionic attraction or repulsion, and the formation of homomeric and heteromeric coiled coils can be controlled by exploiting these properties (O'Shea et al., 1992, 1993; Graddis et al., 1993; Monera et al., 1993, 1994; Zhou et al., 1994; Myszka & Chaiken, 1994).

The hydrophobic interface of many leucine zippers is interrupted by a pair of Asn residues at a central *a* position. This partially destabilizes the coiled coil and constrains the helices to be parallel and in register (Alber, 1992). In the absence of a central Asn pair, mutations at *a* and *d* of GCN4-

† This work was supported in part by the Swiss National Science Foundation.

‡ Biochemisches Institut der Universität Zürich.
§ Universitätsspital.
|| Institut für Polymere.

⊗ Abstract published in *Advance ACS Abstracts,* March 1, 1995.

[1] GCN4-p1 corresponds to the C-terminal sequence 249−281 of GCN4 (O'Shea et al., 1989).

0006-2960/95/0434-4097$09.00/0

p1 can produce trimeric and tetrameric coiled coils (Harbury et al., 1993). For example, the variant of GCN4-p1 with Ile at every *a* and *d* position is a three-stranded coiled coil (Harbury et al., 1994). Leu at *a* and Ile at *d* results in a four-stranded zipper (Harbury et al., 1993). Clearly, the shape and packing of aliphatic side chains at *a* and *d* influence the number of strands that can be accommodated in the coiled coil.

Although a detailed understanding of the many factors influencing the thermodynamic stability of leucine zippers and the specificity of their assembly has been acquired, very little is known about the kinetics of leucine zipper folding. Dimerization and strand exchange of the Fos-Jun leucine zipper occurs with half-times <10 s (Patel et al., 1994). The very extended coiled coil in tropomyosin is formed through rapid association of monomeric chains followed by a slow unimolecular reorganization to the final native structure (Mo et al., 1991; Ozeki et al., 1991). Unlike the coiled coil domain of tropomyosin, which is very long and very stable, the short leucine zipper domains of transcription factors must associate and dissociate repeatedly to accomplish their function. Since, in a single cell, the number of transcription factors is likely to be very small, the specificity of association and dissociation of leucine zipper domains may be determined kinetically rather than by equilibrium thermodynamics. Therefore, a thorough understanding of the kinetics of association, dissociation, and exchange of strands between leucine zippers is of prime importance. In addition to these functional considerations, the study of leucine zipper folding provides an excellent model of the folding and assembly of a well-defined regular structure from randomly coiled polypeptide chains.

We have recently introduced a fluorescence stopped flow method for following the kinetics of leucine zipper folding. The approach was applied to GCN4-p1, the folding of which was shown to proceed through one or more intermediate steps (Wendt et al., 1994). The principle of the method, which involves chemically linking a fluorescent group to the N-terminus of the peptide, is that fluorescence is quenched in the parallel coiled coil, in which the fluorescent groups are close to each other, and that fluorescence intensity increases when the chains dissociate. Here we have used the fluorescence quenching approach to investigate the kinetics of folding of five model leucine zipper peptides. Residues at an *a* and/or *d* position were mutated to modulate the stability of the coiled coils. The time course of strand exchange between coiled coils could be determined by mixing fluorescent and nonfluorescent peptides, and the reversible kinetics of association and dissociation were analyzed by following the rate of relaxation after rapid perturbation of a preexisting monomer $\leftrightarrows$ coiled coil equilibrium.

MATERIALS AND METHODS

Peptide Synthesis and Purification. Peptides were synthesized on an Applied Biosystems synthesizer model 430 A, using the Fmoc protection strategy and the Rapid Amide resin from DuPont. Fluorescent groups were coupled to the free α-amino group of the variant of the peptide that had three additional N-terminal glycine residues. 5-(and 6)-Carboxyfluorescein (Flu)[2] was introduced by reaction with 5-(and 6)-carboxyfluorescein-*N*-hydroxysuccinimidyl ester (Molecular Probes, Eugene, OR). Coupling with [7-dimethylaminocoumarin-(4)] acetic acid (Daca)[2] (Molecular Probes) was performed as follows: 60 μmol of Daca in 1 mL of dimethylformamide was preactivated with 60 μmol of diisopropylcarbodiimide for 5 min in the dark, and the solution was allowed to react with the resin-bound peptide (ca. 20 μmol) for 2 h at room temperature in the dark. Completion of the reaction was checked by the Kaiser test (Kaiser et al., 1970). Where necessary, the N-terminal residue was acetylated by reaction with a 20-fold molar excess of acetic anhydride and a 10-fold molar excess of triethylamine in dimethylformamide. Deprotection and cleavage from the resin was performed with a mixture of 0.375 g of phenol in 5 mL of trifluoroacetic acid + 0.25 mL of H_2O, as recommended by the manufacturer, and the peptides were released as the C-terminal amides. The material was desalted on a Sephadex G-25 column in 1 M acetic acid. Final purification was achieved by reversed-phase HPLC on a semipreparative C_8 column (Macherey and Nagel) eluted with binary gradients of acetonitrile/H_2O containing 0.1% or 0.085% trifluoroacetic acid. The purity of the peptides was confirmed by amino acid analysis and ion spray mass spectrometry. Peptides were found to be >95% pure. Peptide concentrations were determined by amino acid analysis on a Biotronik LC 6001 amino acid analyzer using orthophthalaldehyde derivatization.

Buffer. All experiments were performed in 0.1 M sodium phosphate buffer, pH 7.2, unless otherwise stated.

CD Spectroscopy. CD spectra were measured on a JASCO J-500 C spectropolarimeter at 20 °C and at a scan speed of 1 nm/min. Denaturation curves were measured at a constant wavelength in cuvettes of 2 mm pathlength. Appropriate concentrations of urea were prepared by serial dilution of 3, 6, or 9 M urea stock solutions (prepared gravimetrically) with buffer. For each data point 25 μL of peptide stock solution (1.08 mM) was diluted into 975 μL of the appropriate urea concentration. The peptide/urea solutions were equilibrated at 20 °C for about 30 min. Data analysis was performed according to Pace (1986). Correction was made for a slight linear dependence of θ_0 and θ_{max} on urea concentration (Pace et al., 1989; Jackson et al., 1993).

Fluorescence Spectra. A Spex Fluorolog spectrofluorimeter was employed, and cuvettes of 1 cm pathlength and a minimal volume of 2 mL were used. Spectra were measured in 1 nm steps with 2 s integration time. The slow strand exchange between Flu-LZ and Ac-LZ was measured on an Aminco SPF 500 spectrofluorimeter.

Stopped Flow Measurements. Measurements were made on an SF-61 stopped flow spectrofluorimeter with a dead time of 1 ms (High Tech Scientific Ltd., Salisbury, U.K.). Excitation was at 492 nm, and emission was measured above 530 nm (cut-off filter OG530). Apparent rate constants were averaged from 6−10 single measurements, using the software provided by High Tech Scientific. All experiments were performed at 25 °C. Control experiments were performed with peptide LZ(7P14P), which is random coiled an does not associate to a coiled coil in the micromolar concentration range (Leder et al., 1994). No time-dependent change of

[2] Abbreviations: Daca, [7-dimethylaminocoumarin-(4)] acetic acid; Flu, 5-(and 6)-carboxyfluorescein; Fmoc, 9-fluorenylmethoxycarbonyl.

Table 1: Sequence of Leucine Zipper Peptides[a]

abbreviation	sequence[a]
	1 5 9 12 16 19 23 26
LZ	X_0-EYEALEKKLAALEAKLQALEKKLEALEHG-NH_2
	abcdefga d a d a d
LZ(12A)	.....A.....
LZ(16A)	.....A.....
LZ(12A16A)	.....A...A.....
LZ(16N)	.....N.....
LZ(7P14P)	.....P.....P.....

[a] X_0 = N^{α}-acetyl (Ac), fluorescein-GGG (Flu), or [7-dimethylaminocoumarin-(4)]-acetyl-GGG (Daca).

the fluorescence signal was observed when Flu-LZ(7P14P) was mixed with Ac-LZ(7P14P) and when Flu-LZ(7P14P) was diluted with buffer.

Sedimentation Equilibrium. Conventional sedimentation equilibrium measurements were made on a Beckman Optima XL-A analytical ultracentrifuge equipped with variable absorbance optics. Standard Kel-F double sector cells were loaded with a sample volume of 120 μL with the fluorocarbon oil FC43 being used to provide a false bottom. Sample concentrations used were between 5 and 50 μM, and each sample was centrifuged at several different speeds in the range of 16 000−40 000 rpm. It was established that the equilibrium condition was reached within 24 h. Twenty accumulations were averaged per data point at a radial spacing of 0.001 cm, and the absorbance versus radial position data obtained were analyzed in the standard fashion using software provided by the instrument manufacturer. All measurements were carried out at 20 °C in an aqueous buffer containing 0.01 M sodium phosphate and 0.09 M sodium chloride, pH 7.2. Partial specific volumes were calculated from the amino acid composition (Laue et al., 1992), and values of $v_{20,c}$ = 0.762 and $v_{20,c}$ = 0.756 mL g^{-1} were obtained for LZ and LZ(16A), respectively.

RESULTS

Leucine Zipper Model Peptides. The peptides used in this study were modeled on a sequence designed to probe the helix-forming propensity of amino acids (O'Neil & DeGrado, 1990). The structure of one of these peptides has been determined crystallographically and shown to be a three-stranded coiled coil in which two strands run parallel and the third antiparallel (Lovejoy et al., 1993). The sequence that the present study is based on consisted of four similar peptide heptads following an N-terminal Glu residue and was termed peptide LZ. An elongated variant of LZ with three additional glycine residues was chemically modified by the addition of a fluorescent label. The stability of the coiled coil structure formed by these peptides could be modulated by single or double Leu/Ala or Leu/Asn substitutions in the hydrophobic core. The sequences are listed in Table 1.

Peptide Ac-LZ assembles to a coiled coil that is predominantly trimeric in the micromolar concentration range, as was shown by sedimentation equilibrium analysis in the ultracentrifuge. In the concentration range of 5−50 μM, peptide Ac-LZ sedimented with an apparent mass of 9500 ± 500 Da, assuming sedimentation of a single homogeneous species. In contrast, the less stable derivatives with substitutions at positions 12 and/or 16 are predominantly dimeric in the micromolar concentration range. For example, 7 μM peptide Ac-LZ(16A) sedimented with an apparent mass of 5700 ± 110 Da, a value slightly lower than the calulated dimer mass of 6528 Da. The CD-signal at 222 nm of 7 μM Ac-LZ(16A) was −24 000 deg cm^2 $dmol^{-1}$. This value amounts to 82% of the extrapolated maximum CD signal of the coiled coil conformation of this peptide (see $\Delta\theta_{max}$ in Table 2). Even though Ac-LZ(16A) and Ac-LZ(12A) form trimers at higher concentrations (see Discussion), the values of the ellipticity and the apparent mass indicated that the monomer ⇆ dimer equilibrium dominated below 5 μM peptide where all the kinetic experiments described below were performed.

Urea Denaturation and Monomer ⇆ Dimer Equilibrium. The thermodynamic stability of the peptides was assessed from the results of urea induced unfolding experiments. Figure 1 shows the denaturation curves obtained by monitoring the change in peptide ellipticity at 222 nm (θ_{222}) as a function of urea concentration. The unfolding midpoint, $[urea]_{50}$, of 2.5 μM Ac-LZ was 5.7 M urea whereas Leu/Ala substitutions at the central a_{16} and/or d_{12} position(s) or the replacement of Leu_{16} by Asn shifted the unfolding midpoint to lower urea concentration. Values of $[urea]_{50}$ depended on peptide concentration, as it was expected for the monomer ⇆ coiled coil equilibria (not shown).

In view of the data from the sedimentation equilibrium analysis, the unfolding curves of Ac-LZ(12A), Ac-LZ(16A), Ac-LZ(12A16A), and Ac-LZ(16N) were analyzed as a two-state transition in which only the native dimeric coiled coil, D, and the denatured monomeric peptide, M, are stable:

$$M + M \leftrightarrows D$$

The equilibrium constant of unfolding, $K_{d,U}$, is defined as

$$K_{d,U} = [M]^2/[D] = 2[M_0]f_m^2/(1 - f_m) \quad (1)$$

where $[M_0]$ is the total peptide concentration and f_m the fraction of the peptide in the monomeric form. f_m is obtained from the change of the CD signal by

$$f_m = 1 - \Delta\theta/\Delta\theta_{max} \quad (2)$$

$\Delta\theta = \theta - \theta_0$, where θ is the measured ellipticity and θ_0 is the ellipticity of the unfolded monomer, which was taken to be 2500 deg cm^2 $dmol^{-1}$ (Scholtz et al., 1991). $\Delta\theta_{max} = \theta_{max} - \theta_0$, where θ_{max} is the ellipticity of the folded dimer. The free energy of unfolding, ΔG_U, is given by

$$K_{d,U} = \exp(-\Delta G_U/RT) \quad (3)$$

Values of ΔG_U^w, the free energy change on unfolding in water, were obtained by the linear extrapolation of plots of ΔG_U versus [urea] to 0 M urea (Pace, 1986) and the results listed in Table 2.

Dissociation Constants Determined from the Concentration Dependence of θ_{222}. The monomer ⇆ dimer equilibrium can be followed by the change in θ_{222} as a function of peptide concentration. Plots for Ac-LZ(12A) and Ac-LZ(16N) are shown in Figure 2. The fact that the signal is concentration dependent clearly indicates that both monomers and dimers are present at equilibrium. The dissociation constant $K_{d,CD}$

Table 2: Thermodynamic Stability of Leucine Zippers and the Dissociation Constants of Monomer ⇄ Dimer Equilibria Calculated from (i) Denaturation Curves ($K_{d,U}$), (ii) Concentration Dependence of CD ($K_{d,CD}$), and (iii) Concentration Dependence of Fluorescence ($K_{d,F}$)

peptide	ΔG_U^w [a] (kJ/mol)	$K_{d,U}$ [b]	[urea]$_5$ [c] (M)	$K_{d,CD}$ [d] (μM)	$\Delta\theta_{max}$ [d] (deg cm^2 dmol^{-1})	$K_{d,F}$ [f] (μM)	% maximum quenching [g]
LZ	nd	nd	5.7	nd	32 500 [e]	nd	nd
LZ(12A)	38	0.2	3.0	1.3 ± 0.5	31 700	0.7 ± 0.3	~95
LZ(16A)	36	0.4	2.6	1.1 ± 0.6	29 100	2.3 ± 0.7	~95
LZ(12A16A)	32	3.9	1.9	4.0 ± 1.2	17 900	nd	nd
LZ(16N)	37	0.5	1.6	1.2 ± 0.6	26 500	2.4 ± 0.6	~85

[a] From the linear extrapolation of ΔG_U versus [urea] to 0 M urea (Pace, 1986). Because unfolding began at very low [urea] and there was very little baseline for the folded form (Figure 1), calculation of ΔG_U^w was prone to a large error. [b] Because of the large error of ΔG_U^w, the error of $K_{d,U}$ is likely to be larger than the error of $K_{d,CD}$ and $K_{d,F}$. [c] Estimated from Figure 1. [d] Data of Figure 2 analyzed according to eq 4. [e] Measured value for 27 μM peptide concentration. [f] Calculated according to eq 6. The value of α in eq 6 was determined from the concentration dependence of the fluorescence of Flu-LZ(7P14P), which does not dimerize. [g] Calculated as $100 \times \beta/2\alpha$ (eqs 5 and 6).

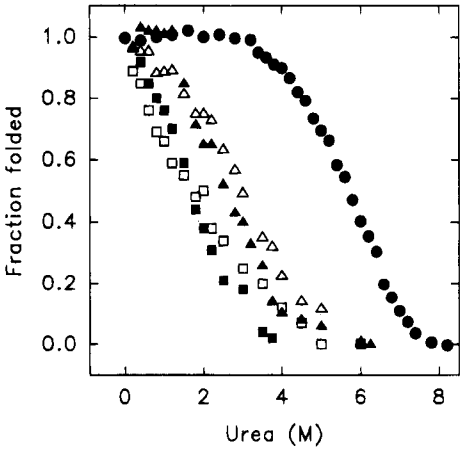

FIGURE 1: Unfolding of peptides in urea. The ellipticity at 222 nm was followed as a function of urea concentration. Fraction folded was determined as described in the text. Ac-LZ (●), Ac-LZ(12A) (△), Ac-LZ(16A) (▲), Ac-LZ(12A16A) (□), Ac-LZ(16N) (■). Total peptide concentrations were 27 μM, except for Ac-LZ which was 2.5 μM.

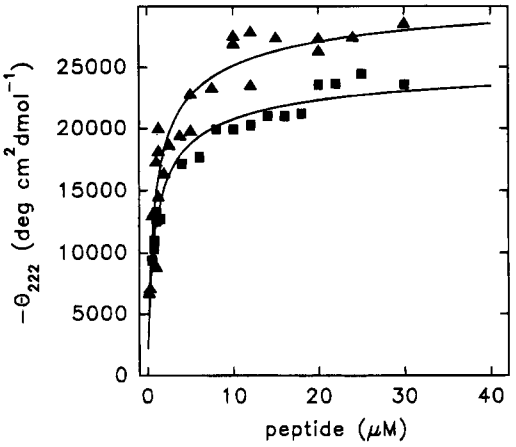

FIGURE 2: Concentration dependence of θ_{222} for Ac-LZ(12A) (▲) and Ac-LZ(16N) (■). Solid lines are best fits according to eq 4 for $K_{d,CD}$ = 1.3 μM, $\Delta\theta_{max}$ = 31 700 deg cm^2 dmol^{-1} (▲); $K_{d,CD}$ = 1.2 μM, $\Delta\theta_{max}$ = 26 500 deg cm^2 dmol^{-1} (■). θ_0 of the unfolded peptide was fixed at 2500 deg cm^2 dmol^{-1} (Scholtz et al., 1991).

can be calculated from

$$K_{d,CD} = 2[M_0](1 - \Delta\theta/\Delta\theta_{max})^2/(\Delta\theta/\Delta\theta_{max}) \quad (4)$$

Equation 4 follows from eqs 1 and 2. The concentration dependence of θ_{222} was analyzed for $K_{d,CD}$ and $\Delta\theta_{max}$ (eq 4) and the results listed in Table 2. $K_{d,U}$ and $K_{d,CD}$ are in reasonable agreement, indicating that the change of the CD

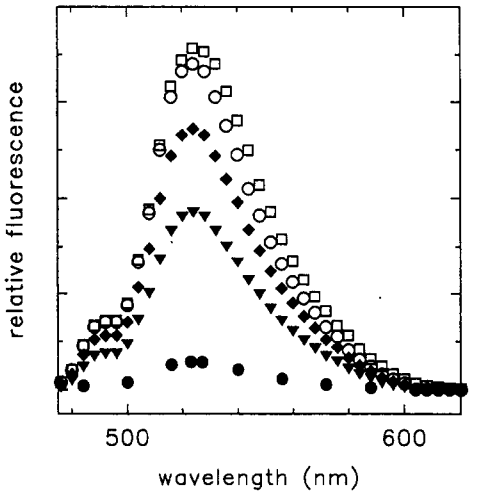

FIGURE 3: Fluorescence emission spectra (excitation 490 nm) of 2 μM solutions of Flu-LZ (●), Flu-LZ(16A) (▼), Flu-LZ(12A16A) (◆), Flu-LZ(7P14P) (□), and Flu-LZ in 8 M urea (○).

signal observed on denaturation and on changing the peptide concentration relates to the same equilibrium reaction. $\Delta\theta_{max}$ values in Table 2 may be compared to the $\Delta\theta_{max}$ of an ideal α-helix, calculated to be −31 500 deg cm^2 dmol^{-1} (Scholtz et al., 1991). On the basis of this theoretical maximum, trimeric Ac-LZ and dimeric Ac-LZ(12A) are 100% helical. The helix contents of Ac-LZ(16A), Ac-LZ(16N), and Ac-LZ(12A16A) are 93%, 84%, and 57%, respectively. Two Leu/Ala or a single Leu/Asn substitution significantly interfere with the regular helical structure of the coiled coil. (If the extrapolated θ_{max} value indicates <100% helix content, it does not mean that the coiled coil is at equilibrium with a substantial amount of monomeric chain, but that the coiled coil is not composed of ideal α-helices.)

Fluorescent Labeled Peptides. Flu or Daca groups were coupled via a triglycine spacer to the N-terminal Glu of the peptides (Table 1). The spacer ensures that the fluorescent group does not interfere with the folding of the coiled coil. It has been shown that a fluorescein group attached in this way does not alter the K_d of the monomer ⇆ dimer equilibrium in GCN4-p1 (Wendt et al., 1994).

A 2 μM solution of Flu-LZ fluoresces weakly with an emission maximum at 525 nm (Figure 3). Emission increases tenfold in 8 M urea. The magnitude and shape of the emission spectrum of denatured Flu-LZ are nearly indistinguishable from those of the spectrum of Flu-LZ-(7P14P). This is a peptide that differs from Flu-LZ by Lys/Pro and Ala/Pro substitutions in positions 7 and 14, respectively, positions that are exposed to the solvent in the

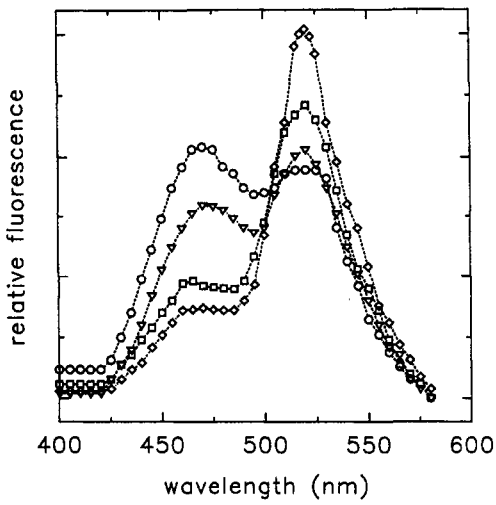

FIGURE 4: Mixing of Flu-LZ and Daca-LZ induces the formation of heteromeric (Daca,Flu)-LZ as is revealed by a time-dependent appearance of fluorescence energy transfer from Daca to Flu. Equal volumes of 2 μM Daca-LZ and 2 μM Flu-LZ were mixed and the fluorescence spectra recorded at 45 s (○), 5 min (▽), 40 min (□), and 2 h (◇) after mixing. Excitation was at 380 nm.

coiled coil. Ac-LZ(7P14P) exhibits a random coil CD spectrum (Leder et al., 1994). The near identity of the fluorescence spectra of denatured Flu-LZ and Flu-LZ(7P14P) demonstrates that the change of fluorescence is solely due to unfolding of the coiled coil. This is supported by the fact that Flu-LZ(16A) and Flu-LZ(12A16A), which are partly unfolded at 2 μM concentration, show higher fluorescence than Flu-LZ at this concentration (Figure 3).

Since Flu-LZ is trimeric, two strand alignments are possible: three strands running parallel or two running parallel and one antiparallel. In the latter arrangement one of the fluorophores would be expected to fluoresce fully while the other two would be quenched and, in this case, the maximal predicted change in fluorescence on strand separation would be an increase in emission by a factor of three. The 10-fold increase of fluorescence emission observed upon unfolding therefore indicates that the three strands must run parallel.

Further to demonstrate the proximity of the fluorophores in the coiled coil, equal amounts of Flu-LZ and Daca-LZ were mixed, and the fluorescence emission spectrum, following excitation of Daca at 380 nm, was recorded regularly over a period of 2 h (Flu absorbs minimally at this excitation wavelength). The emission intensity at 475 nm (due to Daca) decreases while there is a parallel increase in emission intensity at 525 nm originating from the Flu chromophore (Figure 4). This must be due to the formation of heteromeric (Daca,Flu)-LZ, in which Daca functions as a donor, and Flu as an acceptor, fluorophore, producing Förster-type fluorescence energy transfer. No such effect was observed in a control experiment with 2 μM solutions of free fluorophores. Since LZ is a trimer, mixing of Flu-LZ and Daca-LZ produces a mixture of species with Daca/Flu equal to 2:1 or 1:2. As a result, no attempt was made to estimate the distance between the donor and acceptor fluorophores from resonance energy transfer data.

Dissociation Constants Obtained from Fluorescence Quenching. Following the increase of the fluorescence emission as a function of the peptide concentration offers yet another means to calculate a dissociation constant, $K_{d,F}$. The total fluorescence intensity, F, can be expressed as

$$F = \alpha[M] + \beta[D] \quad (5)$$

α and β are the molar fluorescence coefficients of monomer and dimer, respectively. Substituting $[M] = [M_0] - 2[D]$ in eq 5, one obtains $[D] = (F - \alpha[M_0])/(\beta - 2\alpha)$. Substituting these expressions for [M] and [D] in $K_{d,F} = [M]^2/[D]$ leads to

$$4z^2 - z(4n[M_0] + nK_{d,F}) + n^2[M_0]^2 = 0 \quad (6)$$

where $z = F - \alpha[M_0]$ and $n = \beta - 2\alpha$. The concentration dependence of the fluorescence emission was analyzed in this way, yielding $K_{d,F}$. The reasonable agreement between $K_{d,F}$ and $K_{d,CD}$ (Table 2) underlines the previous finding that the fluorescence group does not markedly interfere with the formation of the coiled coil. $K_{d,F}$ of Flu-LZ(12A16A) could not be determined accurately by the fluorescence method because of the inner filter effect at the higher peptide concentrations that were necessary to shift the equilibrium to the side of the dimer.

The Kinetics of Strand Exchange between Leucine Zippers. Mixing of Flu-labeled peptides with nonlabeled peptides (X_0 = acetyl) in an equimolar ratio resulted in a time-dependent fluorescence increase. The increase was caused by the exchange of strands between fluorescently labeled and nonlabeled coiled coils, leading to the formation of dimeric species with an unpaired fluorescence group. In the case of the trimeric LZ, strand exchange produced coiled coils with either one or two Flu groups. Since Flu did not interfere with the monomer ⇆ coiled coil equilibrium, the overall equilibrium did not change during the experiment.

In the interests of clarity, the definitions of the rate constants to be used in the following sections will be given here. Rate constants derived from strand exchange experiments are all denoted by the subscript "ex". Monophasic exchange reactions [as in LZ(16N), LZ(12A16A)] are therefore characterized by the single rate constant k_{ex1}, whereas biphasic processes [as in LZ(16A), LZ(12A)] are described by the two rate constants k_{ex1} and k_{ex2}. k_{ex1} always refers to the faster phase and k_{ex2} to the slower.

The time course of strand exchange between the very stable coiled coils Flu-LZ and Ac-LZ following manual mixing is shown in Figure 5. The rate of exchange was independent of peptide concentration, indicating that the dissociation of the coiled coil, a unimolecular process, was rate limiting, and that concentration-dependent reassociation did not contribute to the overall rate of exchange. Stopped flow mixing experiments revealed that strand exchange between Flu-LZ and Ac-LZ was in fact a biphasic reaction with an initial rapid phase that accounted for only 10−15% of the total amplitude and had a rate constant $k_{ex1} = (2.8 \pm 0.2) \times 10^{-3}$ s^{-1}. The second phase was slow, with $k_{ex2} = (3.0 \pm 0.1) \times 10^{-4}$ s^{-1}.

A single Leu/Ala substitution increased the rate of strand exchange by more than three orders of magnitude. Whereas peptides LZ(12A) and LZ(16A) also showed biphasic kinetics of strand exchange, only a single phase, characterized by the rate constant k_{ex1}, was seen with LZ(12A16A) and LZ(16N). This observation is discussed in the context of the following experiments. Exchange rate constants and amplitudes are listed in Table 3.

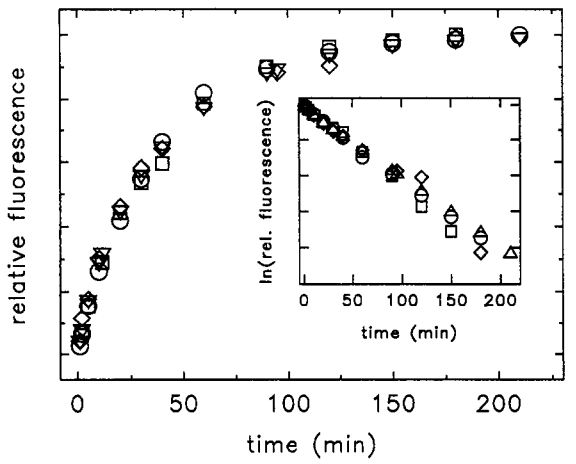

FIGURE 5: Strand exchange between Flu-LZ and Ac-LZ is independent of peptide concentration. Equal volumes of Flu-LZ and Ac-LZ were mixed, and the change in fluorescence intensity was followed at 525 nm (excitation 492 nm). Total peptide concentrations were 19 μM (○), 10 μM (□), 6 μM (◇), 2 μM (△). (Inset) Half-log plot of the data.

Relaxation after Equilibrium Perturbation by Rapid Dilution. To unravel the kinetics of association and dissociation of the leucine zippers, the Flu-labeled peptides were mixed with an equal volume of buffer in the stopped flow apparatus. The fluorescence intensity increased during relaxation to the new equilibrium position, due to the increase in concentration of monomers. If the equilibrium perturbation is relatively small, the rate equation can be linearized, and the rate constants obtained from the concentration dependence of the relaxation time (Bernasconi, 1976).[3] Folding of Flu-LZ could not be followed by the equilibrium perturbation–relaxation procedure as the peptide is essentially 100% trimeric in the micromolar concentration range.

(a) The Folding of Peptides LZ(12A16A) and LZ(16N) Can Be Described by a Simple Two-State Monomer ⇆ Dimer Mechanism. The relaxation process corresponds to a single-exponential decay curve characterized by the relaxation time τ. A minimal mechanism of the folding process is

$$M + M \underset{k_{-1}}{\overset{k_1}{\rightleftharpoons}} D \qquad \text{(mechanism I)}$$

k_1 and k_{-1} were estimated from the concentration dependence of $1/\tau$ according to (Bernasconi, 1976)

$$1/\tau = 4k_1[M_f] + k_{-1} \tag{7}$$

$[M_f]$, the monomer concentration at the final equilibrium after dilution, was calculated from the total peptide concentration $[M_0]$ and $K_{d,F}$ for LZ(16N) or $K_{d,CD}$ for LZ(12A16A). Plots of $1/\tau$ versus $[M_f]$ are shown in Figure 7A and the rate constants in Table 4. As the rate of strand exchange in these two peptides is independent of peptide concentration and obeys a single-exponential reaction, the values of k_{-1} should be the same as the apparent rate constants of the exchange experiments, k_{ex1}, for these two peptides (see Appendix A).

[3] The error introduced by the linearization leads to underestimation of $1/\tau$ when the system relaxes from higher to lower peptide concentration. Estimated errors in $1/\tau$ were in the range −1 to −10% [see Bernasconi (1976), pp 76–84, for approximate percent errors in $1/\tau$ as a function of the maximum deviation from equilibrium and the time range of the measurements].

In fact, the values are indistinguishable within the limits of error (Tables 3 and 4). Furthermore, the dissociation constants calculated from k_{-1}/k_1 are in reasonable agreement with those determined directly (Table 2).

(b) The Folding of Peptides LZ(12A) and LZ(16A) Can Be Described by a Biphasic Mechanism Composed of an Association Reaction Coupled to a Conformational Reorganization. The relaxation process showed two phases. One phase was concentration dependent; the other was concentration independent. A possible mechanism is

$$M + M \underset{k_{-1}}{\overset{k_1}{\rightleftharpoons}} D^* \underset{k_{-2}}{\overset{k_2}{\rightleftharpoons}} D \qquad \text{(mechanism II)}$$

in which the concentration-independent, unimolecular reorganization follows the concentration-dependent, bimolecular association of the polypeptide chains. Alternatively, the conformational reorganization could also take place before the association step (see Discussion). In the case of Flu-LZ(12A) the rate of the fast phase depended on the peptide concentration whereas the rate of the slow phase was apparently concentration independent (Figures 6 and 7B). The reverse was seen with LZ(16A); the rate of the rapid initial phase was apparently concentration independent while that of the second slow phase was concentration dependent (Figures 7C and D).

If the fast relaxation time τ_1 relates to the concentration-dependent reaction step, as it was the case for peptide LZ-(12A), the linearized rate equations for mechanism II are (see Appendix B):

$$1/\tau_1 = 4k_1[M_f] + k_{-1} \tag{8a}$$

$$1/\tau_2 = 4k_1k_2[M_f]/(4k_1[M_f] + k_{-1}) + k_{-2} \tag{8b}$$

If the concentration-independent conformational reorganization is faster than the concentration-dependent association step [peptide LZ(16A)], the linearized rate equations become[4]

$$1/\tau_1 = k_2 + k_{-2} \tag{9a}$$

$$1/\tau_2 = 4k_1[M_f] + k_{-1}k_{-2}/(k_2 + k_{-2}) \tag{9b}$$

Plots of $1/\tau_1$ and $1/\tau_2$ against $[M_f]$ are shown in Figure 7. In the case of Flu-LZ(12A), the rate constants of the association/dissociation reaction, k_1 and k_{-1}, were obtained directly from eq 8a. k_{-1} has to equal k_{ex1}, the rate constant for the fast phase seen in strand exchange experiments with this peptide (see Appendix A). The measured values were in good agreement with each other (Tables 3 and 4). Equation 8b predicts that $1/\tau_2$ depends on peptide concentration. However, the values were considerably scattered and appeared to be independent of $[M_f]$. The reason is that the term $4k_1[M_f]/(4k_1[M_f] + k_{-1})$ in eq 8b is close to unity in the concentration range used in the experiment. The limiting value at high peptide concentration is $1/\tau_2 = k_2 + k_{-2}$, and, furthermore, k_{ex2}, the rate constant for the slow step in the exchange experiments, is approximated by $k_2 + k_{-2}$, as k_{ex2} applies to the second step of mechanism II (see Appendix A). The mean of the five values of $1/\tau_2$ in Figure 7B is 1.3 $\pm$ 0.8 s^{-1}, in fair agreement with $k_{ex2} = 0.7 \pm 0.1$ s^{-1} (Table 3). The dissociation constant of the association step is $k_{-1}/$

[4] τ_1 always refers to the faster, and τ_2 to the slower, relaxation phase.

Table 3: Rate Constants of Strand Exchange between Leucine Zippers[a]

peptide	k_{ex1} (s^{-1})	amplitude (%)	k_{ex2} (s^{-1})	amplitude (%)
LZ	$(2.8 \pm 0.2) \times 10^{-3}$	10−15	$(3.0 \pm 0.1) \times 10^{-4}$	85−90
LZ(12A)	4.4 ± 0.8	59−77	0.7 ± 0.1	23−41
LZ (16A)	34.0 ± 3.2	15−30	0.14 ± 0.1	70−85
LZ (12A16A)	11.5 ± 1.5	100		
LZ (16N)	10.9 ± 1.5	100		

[a] Average of five measurements at 0.5, 1, 2, 3, and 4 μM total peptide concentration. All values were peptide concentration independent.

Table 4: Kinetic Constants for Leucine Zipper Folding Estimated from Rapid Dilution−Relaxation Experiments

peptide	k_1 ($\times 10^6$) (M^{-1} s^{-1})	k_{-1} (s^{-1})	amplitude (%)	$k_2 + k_{-2}$ (s^{-1})	amplitude (%)
LZ (12A16A)[a]	4.0 ± 0.5	12.7 ± 3	100		
LZ (16N)[a]	4.2 ± 0.5	8.6 ± 1.5	100		
LZ(12A)[b]	6.2 ± 0.5	2.3 ± 1.5	82−86	1.3 ± 0.8[d]	14−18
LZ(16A)[b]	0.08 ± 0.03	c	67−69	31.3 ± 1.7	31−33

[a] Mechanism I. [b] Mechanism II. [c] k_{-1} cannot be determined from the data available. [d] Mean of $1/\tau_2$ values (slow phase) in Figure 7B.

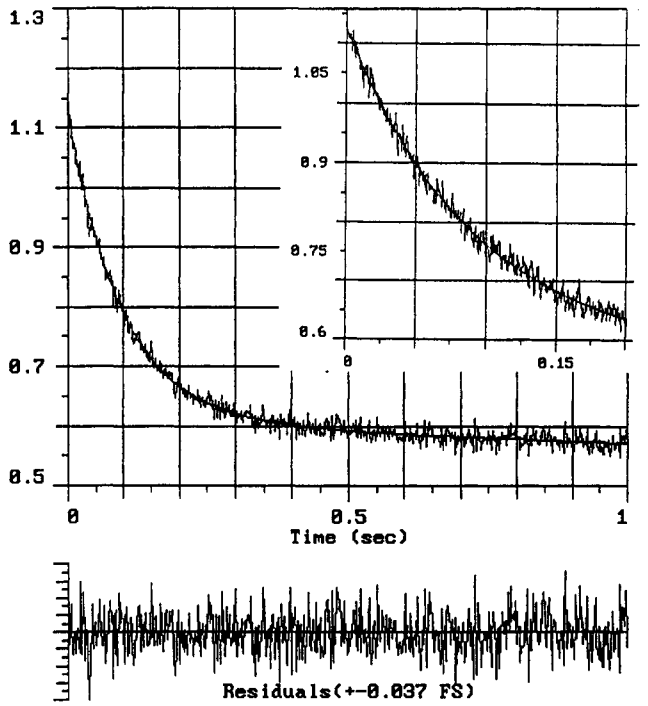

FIGURE 6: Representative example of relaxation after rapid dilution with buffer. A decrease in the signal (volts) corresponds to an increase of fluorescence intensity. The trace is for the relaxation after 1:1 dilution of 1.35 μM Flu-LZ(12A). The solid line is a best fit to $F = A_1 \exp(-t/\tau_1) + A_2 \exp(-t/\tau_2)] + A_\infty$ for $1/\tau_1 = (10.5 \pm 0.38)$ s^{-1}, $1/\tau_2 = (0.688 \pm 0.343)$ s^{-1}, $A_1 = 0.509$, $A_2 = 0.091$, and $A_\infty = 0.525$. (Inset) Initial 200 ms of reaction.

$k_1 = 0.37$ μM. As, for the overall process $K_{d,F} = k_{-1}k_{-2}/k_1k_2 = 0.7$ μM (Table 2), it follows that the equilibrium constant of the conformational reorganization step D* ⇆ D is not far from unity.

In contrast to peptide LZ(12A), the rapid relaxation phase in LZ(16A) appears to be independent of the peptide concentration and therefore $k_2 + k_{-2}$ must equal k_{ex1} (see Appendix A). From eq 9a, $k_2 + k_{-2} = 31.3 \pm 1.7$ s^{-1} (Figure 7C), and, in fact, the numerical equivalence between this value and that for k_{ex1} was impressive (Tables 3 and 4). As is clear from eq 9b, k_{-1} could not be obtained directly from relaxation kinetic measurements. If it was assumed that $k_{-1} = k_{ex2}$ (=0.14 s^{-1}, the rate constant for the slow step in the exchange kinetic experiments, Table 3), and taking the value $k_1 = 0.08$ μM^{-1} s^{-1} calculated from the slope of the plot of $1/\tau_2$ versus $[M_f]$ in Figure 7D (eq 9b), a value of 1.75 μM for the equilibrium constant of the M + M ⇆ D* reaction could be estimated. Again, the equilibrium constant for D* ⇆ D is not far from unity since the overall measured equilibrium constant $K_{d,F}$ is 2.3 μM (Table 2).

A striking difference between the two leucine zippers is seen in the rates of association of monomers. k_1 of Flu-LZ-(12A) is 75-fold higher than k_1 of Flu-LZ(16A), even though the dissociation constants of the monomer ⇆ dimer equilibrium are very similar for both peptides. The difference in the association rates is compensated by a similar difference in the dissociation rates.

Consistency between strand exchange and equilibrium perturbation−relaxation experiments is further supported when the amplitudes of the two reaction steps listed in Tables 3 and 4 are compared. The concentration-independent phase of relaxation experiments was assumed to correspond to the rearrangement step D* ⇆ D. In both LZ(12A) and LZ(16A) this phase was also that which had the smaller amplitude. Similarly, the corresponding strand exchange rate constants, namely, k_{ex2} for LZ(12A) and k_{ex1} for LZ(16A), pertain to the smaller amplitude phase.

DISCUSSION

Thermodynamic Stability of Model Leucine Zippers. Ac-LZ forms a very stable coiled coil. The remarkable loss of stability introduced by a single Leu/Ala substitution seen here confirms earlier work on coiled coil model peptides by Hodges and co-workers (Hodges et al., 1988; Zhou et al., 1992). Molecular dynamics calculations predict a loss of 15 kJ/mol for a single Leu/Ala substitution in a central *d* position of a coiled coil (Zhang & Hermans, 1993). Although the ΔG_U^w values of Ac-LZ(16N) and Ac-LZ(16A) are almost equal, the Leu/Asn substitution in the a_{16} position of the coiled coil shifts the value of $[urea]_{50}$ to lower urea concentration than the Leu/Ala substitution at the same position.

The Number of Strands in the Model Leucine Zippers. At the beginning of the present study, it was assumed that all the model peptides to be studied would form dimeric coiled coils (O'Neil & DeGrado, 1990). In the meantime, however, the structure of a related peptide, called "coil-Ser", has been shown to conform to a three-stranded coiled coil (Lovejoy et al., 1993). It has been confirmed by sedimentation equilibrium analysis that the peptide Ac-LZ is also mainly

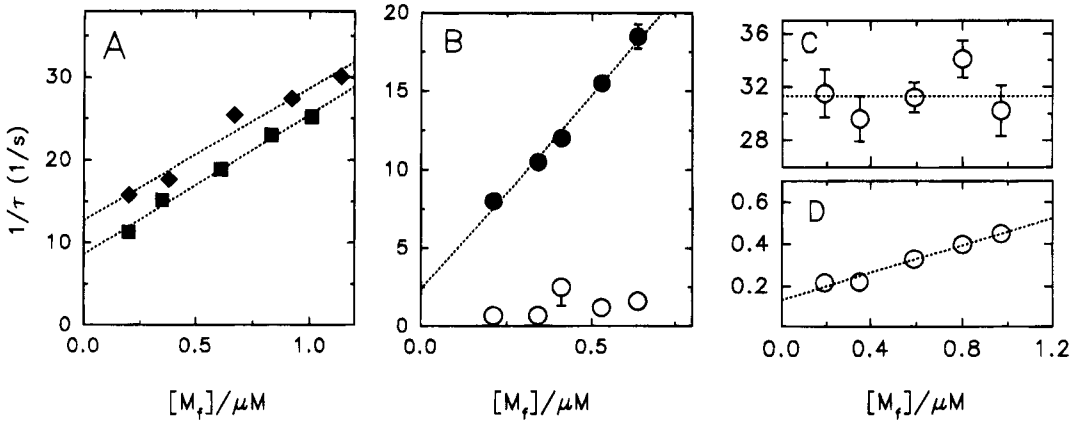

FIGURE 7: Concentration dependence of $1/\tau$ in rapid dilution–relaxation experiments. (A) Flu-LZ(12A16A) (◆) and Flu-LZ(16N) (■). Dashed line is best fit according to eq 7. (B) Flu-LZ(12A), fast phase (●), slow phase (○). Dashed line is best fit according to eq 8a. (C) Flu-LZ(16A), fast phase. Dashed line is best fit according to eq 9a. (D) Flu-LZ(16A), slow phase. Dashed line is best fit according to eq 9b. Values of $1/\tau$ are the mean of 6–10 measurements. Unless indicated, the SEM was smaller than the symbol.

trimeric. Moreover, the 10-fold fluorescence increase upon unfolding of Flu-LZ indicates that the three strands are oriented in a parallel fashion, unlike the "up-up-down" arrangement observed in the "coil-Ser" peptide, for which the parallel arrangement is thought be energetically less favorable because it would result in a Trp-Trp-Trp layer at the first *a* position (position 2), resulting in a steric clash (Lovejoy et al., 1993). Position 2 of peptide LZ is Tyr. The smaller size of Tyr seems to be compatible with an all parallel orientation of the three helices.

In the micromolar concentration range, the less stable derivatives of peptide LZ are predominatly in a monomer ⇆ dimer equilibrium. This equilibrium is the basis of our kinetic experiments. However, peptides LZ(12A) and LZ-(16A), but not LZ(16N), can form trimers at much higher concentration, as can be shown by electrospray mass spectrometry.[5] Although the concentration of trimers was negligible at concentrations below 5 μM where the kinetic experiments have been conducted, the formation of trimers is a potential complication of the kinetic analysis. Mechanisms I and II are approximations that are legitimate only in the low concentration range of a monomer ⇆ dimer ⇆ trimer folding equilibrium.

It has been conjectured that the single Asn found in the hydrophobic core of many naturally occurring leucine zippers serves to constrain the chains to a dimeric, parallel conformation (O'Shea et al., 1991; Alber, 1992). Recent crystal structures of leucine zippers demonstrate that the number of strands in a coiled coil is delicately balanced by the shape and packing of residues in the core (O'Shea et al., 1991; Harbury et al., 1994). A switch in the "strandedness" of coiled coils may have physiological significance, and substitutions in the hydrophobic core might modify the equilibrium between monomers, dimers, trimers, and perhaps higher order oligomers in the physiologically significant micromolar concentration range.

Strand Exchange between Coiled Coils. The high stability of the trimeric coiled coil LZ is reflected by its relatively slow strand exchange with half-time around 30 min (Figure 5), although this rate is still orders of magnitude faster than strand exchange between the very long coiled coils of tropomyosin (Ozeki et al., 1991). The rate of strand exchange is limited by the rate of dissociation of the coiled coil and not by the rate of reassociation of the chains, which is rapid. A mechanism in which coiled coils exchange strands directly can be eliminated, as such an exchange mechanism would have to depend on peptide concentration. The fast and slow exchange rate constants for peptide LZ may correspond to the dimer ⇆ trimer and the monomer ⇆ dimer equilibrium, respectively. Molecular dynamics calculations indicate a lower free energy change for the dimer ⇆ trimer equilibrium than for the monomer ⇆ dimer equilibrium (Lovejoy et al., 1993). However, the biphasic exchange reactions observed with peptides LZ(12A) and (16A) are not due to a monomer ⇆ dimer ⇆ trimer equilibrium, as these peptides do not associate to trimers in the concentration range of our experiments. A possible explanation for the observed kinetic process became clear only from the rapid dilution–relaxation experiments.

The less stable derivatives of peptide LZ exchange strands with half-times ≈1 s. A similarly fast exchange rate was observed for the Fos–Jun pair, the only other leucine zipper for which the kinetics of strand exchange has been measured (Patel et al., 1994). Interestingly, strand exchange is very strongly inhibited when Fos–Jun binds to its target DNA (Patel et al., 1994).

Kinetics of Folding from Rapid Dilution–Relaxation Experiments. Assembly of polypeptides to oligomeric proteins is usually studied by denaturation/renaturation experiments [see for a recent example Milla and Sauer (1994)]. The rapid dilution–relaxation technique was chosen since this method strictly monitors the monomer ⇆ coiled coil equilibrium without introducing complications due to the changes in the solvent in going from the denaturant solution to benign buffer conditions.

The folding of Flu-LZ(12A16A) and Flu-LZ(16N) obeys the simple two-state mechanism I, and the peptides are in a very rapid equilibrium between monomer and dimer. The half-time of folding of these peptides at a concentration of 1 μM is less than 100 ms. The association rate constant of 4×10^6 M^{-1} s^{-1} (Table 4) may be only 2–3 orders of magnitude below the diffusion limit. Folding of the Fos–Jun leucine zipper attached to the basic DNA binding sequence occurs with half-times below 10 s (Patel et al.,

[5] Ionization of 0.1 mM solutions of peptides Ac-LZ(12A) and Ac-LZ(16A) at pH 6 by "soft" desorption–ionization produces a small signal at a mass/charge ratio characteristic for trimers (H. Wendt, E. Dürr, M. Przybylski, and H. R. Bosshard, manuscript in preparation).

1994), and the folding of the P22 Arc repressor provides another example of a very rapid association of a homodimer from unfolded polypeptide chains (Milla & Sauer, 1994). Dimerization of P22 Arc proceeds at an apparent rate similar to that observed here for Flu-LZ(12A16A) and Flu-LZ(16N).

The helices of a leucine zipper are stable only when folded in the coiled coil conformation and not as individual monomeric peptide chains ($\Delta\theta_{222}$ extrapolates to ≈ 0 at low peptide concentration, see Figure 2). Therefore, it is difficult to see how two unfolded polypeptide chains can associate to a coiled coil in a single step. Monomers may collide, perhaps in a partially helical state, to form a dimeric intermediate, which then equilibrates in a monomolecular reaction to the final native coiled coil. The two-state mechanism I adequately describes the kinetic results but may be too simplistic in view of structural considerations.

The folding of Flu-LZ(12A) and Flu-LZ(16A) was more complicated. Mechanism II fitted the experimental results, although, in principle, the concentration-independent, monomolecular step could as well precede the concentration-dependent association step. There is, however, one difficulty in putting the monomolecular before the bimolecular reaction. Fluorescence quenching is caused by two adjacent fluorescein groups in the parallel coiled coil. If a monomeric molecular rearrangement were to take place prior to the association step, the microenvironment of a lone Flu group would have to change substantially to lead to the observed change of fluorescence. This seems difficult to accept since the monomeric chains are essentially random coils. Additionally, it is hard to understand why only monomeric Flu-LZ(12A) and Flu-LZ(16A), but not monomeric Flu-LZ(12A16A) and Flu-LZ(16N), should adopt two different monomeric conformations. In the model envisaged by the two-step mechanism II, D* and D differ with respect to the microenvironment of the two Flu groups. D* may be in a less constrained conformation while D may be more conformationally organized, quenching being stronger in the latter case. The smaller amplitude of the unimolecular reorganization step as compared to the association/dissociation step is in accord with such an interpretation. Depending on delicate differences of interaction in the hydrophobic core, only the more stable derivatives LZ(12A) and LZ(16A) are capable of adopting the two different dimeric conformations, whereas the interchain interaction in the less stable dimers of Flu-LZ(12A16A) and Flu-LZ(16N) is weaker. In line with this interpretation, θ_{max} of the latter two peptides is lower, as is the extent of fluorescence quenching in Flu-LZ(16N) (Table 2). It is, however, also possible that the dimer rearrangement transitions of Flu-LZ(12A16A) and Flu-LZ(16N) are too fast to be measured.

We wish to emphasize that these considerations are speculative and that the experimental approaches used here were incapable of establishing whether monomolecular rearrangement occurred before or after the bimolecular association reaction. However, the following general conclusions can be drawn from our kinetic experiments. First, except in the case of the very stable trimeric coiled coil peptide LZ, association and dissociation of the model leucine zippers is fast and monomers and dimers are in rapid equilibrium. Second, thermodynamic destabilization of the leucine zipper by Leu/Ala and Leu/Asn substitutions not only increases the overall rate of folding but also can change the association and dissociation rates in a position-dependent manner. Finally, except for peptide LZ, the thermodynamic stability of the model leucine zippers in the present study are of a similar magnitude as those of some naturally occurring leucine zipper domains of transcription factors (Alber, 1992; Wendt et al., 1994). Therefore, these results could indicate that, *in vivo*, leucine zipper domains of transcription factors may be constantly associating and dissociating and freely exchanging strands.

APPENDIX A

In the case of mechanism I [peptides LZ(12A16A) and LZ(16N)] the following equilibria are established after mixing of equivalent amounts of fluorescent labeled (subscript "F") and unlabeled peptides

$$\begin{aligned} M + M &\leftrightarrows D \\ M_F + M_F &\leftrightarrows D_{FF} \\ M_F + M &\leftrightarrows D_F \end{aligned} \qquad (1)$$

The equilibrium constants are indistinguishable since the fluorescent group does not measurably interfere with dimer formation. Formation of D_F, which contains an unpaired fluorescent group and is responsible for the fluorescence increase observed in the strand exchange experiment, can be expressed by

$$dD_F/dt = k_1 M M_F - k_{-1} D_F \qquad (2)$$

(Square brackets denoting concentration have been omitted for simplicity). Integration leads to

$$D_F = A - A \exp(-k_{-1}t) \qquad (3)$$

where $A = k_1 M M_F / k_{-1}$. Since the equilibrium constants of eq 1 are the same, the concentrations of M and M_F are equal (mixing of equivalent amounts of labeled and unlabeled peptide) and constant throughout the strand exchange reaction. Therefore, A of eq 3 is also constant and the formation of D_F is governed solely by the exponential term $\exp(-k_{-1}t)$ of eq 3. Hence, the measured rate constant of strand exchange, k_{ex1}, must equal k_{-1}.

In the case of mechanism II [peptides LZ(12A) and LZ(16A)], the following equilibria are established after mixing of fluorescent labeled and unlabeled peptides:

$$\begin{aligned} M + M &\leftrightarrows D^* \leftrightarrows D \\ M_F + M_F &\leftrightarrows D_{FF}^* \leftrightarrows D_{FF} \\ M_F + M &\leftrightarrows D_F^* \leftrightarrows D_F \end{aligned} \qquad (4)$$

If the concentration-dependent and the concentration-independent phases are sufficiently separated, they can be treated as being independent of each other. Relaxation times differed by one order of magnitude for peptide LZ(12A), and by two orders of magnitude for peptide LZ(16A), justifying independent treatment of the two phases. The formation of D_F^* can thus be approximated by eq 3 and hence $k_{-1} \simeq k_{ex1}$ for LZ(12A) and $k_{-1} \simeq k_{ex2}$ for LZ(16A).

By the same reasoning, the concentration-independent reorganization, which also contributes to the change of fluorescence, can be described by

$$dD_F/dt = k_2D_F^* - k_{-2}D_F \quad (5)$$

which integrates to

$$D = B(1 - B\exp[-(k_2 + k_{-2})t]) \quad (6)$$

where $B = k_2(D_F + D_F^*)/(k_2 + k_{-2})$. Since the two phases were strongly separated, $D_F + D_F^* \simeq$ constant during the time that was necessary to establish the equilibrium $D_F^* \leftrightarrows D_F$. Hence, the rate of conformational equilibration is governed only by the term $\exp[-(k_2 + k_{-2})t]$ of eq 6, and $k_2 + k_{-2} \simeq k_{ex2}$ for LZ(12A), and $k_2 + k_{-2} \simeq k_{ex1}$ for LZ(16A).

APPENDIX B

The linearized rate eqs 8a,b and 9a,b of the main text are derived following the general procedure described in chapters 2 and 3 of Bernasconi (1976). The rate equations for mechanism II of the main text are

$$M + M \underset{k_{-1}}{\overset{k_1}{\rightleftharpoons}} D^* \underset{k_{-2}}{\overset{k_2}{\rightleftharpoons}} D$$

are

$$dM/dt = k_{-1}D^* - k_1M^2 \quad (1)$$

$$dD^*/dt = k_1M^2 + k_{-2}D - (k_{-1} + k_2)D^* \quad (2)$$

$$dD/dt = k_2D^* - k_{-2}D \quad (3)$$

(Square brackets denoting concentration have been omitted for simplicity). We substitute the concentrations by the sum of the final concentrations (subscript f) and the concentration changes (symbol Δ):

$$M = M_f + \Delta M \quad (4)$$

$$D^* = D^*_f + \Delta D^* \quad (5)$$

$$D = D_f + \Delta D \quad (6)$$

Insertion of (4−6) in (1−3):

$$d\Delta M/dt = k_{-1}(D^*_f + \Delta D^*) - k_1(M_f + \Delta M_f)^2 \quad (7)$$

$$d\Delta D^*/dt = k_1(M_f + \Delta M)^2 + k_{-2}(D_f + \Delta D) - (k_{-1} + k_2)(D^*_f + \Delta D^*) \quad (8)$$

$$d\Delta D/dt = k_2(D^*_f + \Delta D^*) - k_{-2}(D_f + \Delta D) \quad (9)$$

For mechanism II we define the following stoichiometric relationship:

$$\Delta D^* = -(1/2)\Delta M - \Delta D \quad (10)$$

Equations 7−9 are mutually dependent. We select eqs 8 and 9 to describe the system, substituting ΔD^* by eq 10:

$$-(1/2)(d\Delta M/dt) - d\Delta D/dt = k_1M_f^2 + 2k_1M_f\Delta M + k_1\Delta M^2 + k_{-2}D_f + k_{-2}\Delta D - k_{-1}D^*_f + (1/2)k_{-1}\Delta M + k_{-1}\Delta D - k_2D^*_f + (1/2)k_2\Delta M + k_2\Delta D \quad (11)$$

$$d\Delta D/dt = k_2D^*_f - (1/2)k_2\Delta M - k_2\Delta D - k_{-2}D_f - k_{-2}\Delta D \quad (12)$$

The terms $k_1M_f^2 - k_{-1}D^*_f$ and $k_{-2}D_f - k_2D^*_f$ of eq 11 and $k_2D^*_f - k_{-2}D_f$ of eq 12 represent dD^*_f/dt and dD_f/dt at the final equilibrium and are = 0. The quadratic term $k_1\Delta M^2$ in eq 11 is negligibly small for relatively small deviations from the equilibrium (condition for linearization of rate equations). We group the terms and introduce the explicit expression for $d\Delta D/dt$ of eq 12 in eq 11:

$$d\Delta M/dt + (4k_1M_f + k_{-1})\Delta M + 2k_{-1}\Delta D = 0 \quad (13)$$

$$d\Delta D/dt = (1/2)k_2\Delta M + (k_2 + k_{-2})\Delta D = 0 \quad (14)$$

Equations 13 and 14 are of the form

$$dx_1/dt + a_{11}x_1 + a_{12}x_2 = 0 \quad (15)$$

$$dx_2/dt + a_{21}x_1 + a_{22}x_2 = 0 \quad (16)$$

with $x_1 = \Delta M$, $x_2 = \Delta D$, $a_{11} = 4k_1M_f + k_{-1}$, $a_{12} = 2k_{-1}$, $a_{21} = (1/2)k_2$, and $a_{22} = k_2 + k_{-2}$.

The sums and products of the coefficients in eqs 15 and 16 are defined as [see eqs 3.51 and 3.52 of Bernasconi (1976)]

$$\sum k = a_{11} + a_{22} = 4k_1M_f + k_{-1} + k_2 + k_{-2} \quad (17)$$

$$\prod k = a_{11}a_{22} - a_{12}a_{21} = 4k_1(k_2 + k_{-2})M_f + k_{-1}k_{-2} \quad (18)$$

The general expressions for the two reciprocal relaxation times are [see eqs 3.49 and 3.50 of Bernasconi (1976)]

$$1/\tau_2 = (1/2)\sum k + [((1/2)\sum k)^2 - \prod k]^{1/2} \quad (19)$$

$$1/\tau_2 = (1/2)\sum k - [((1/2)\sum k)^2 - \prod k]^{1/2} \quad (20)$$

If either $a_{11} \gg a_{22}$ or $a_{11} \ll a_{22}$, i.e., if in practice the two relaxation times differ by a factor of about 5 or more, an approximate analytical expression of $1/\tau_1$, the faster of the two relaxation times, is available. $1/\tau_2$ is then obtained from (see eq 3.56 of Bernasconi)

$$1/\tau_2 = \tau_1\prod k \quad (21)$$

Case A, Represented by Peptide LZ(12A). The concentration-dependent relaxation time is shorter than the concentration-independent relaxation time, i.e., $a_{11} \gg a_{22}$. The approximate analytical solution for the short relaxation time is

$$1/\tau_1 = 4k_1M_f + k_{-1} \quad \text{(eq 8a of main text)}$$

which is the same as eq 7 of the main text pertaining to the simpler mechanism I. From eq 21 follows

$$1/\tau_2 = 4k_1k_2M_f/(4k_1M_f + k_{-1}) + k_{-2} \quad \text{(eq 8b of main text)}$$

Case B, Represented by Peptide LZ(16A). The concentration-dependent relaxation time is longer than the concentration-independent relaxation time, i.e., $a_{11} \ll a_{22}$. The approximate analytical solution for the short, concentration-independent phase is

$$1/\tau_1 = k_2 + k_{-2} \quad \text{(eq 9a of main text)}$$

and with eq 21 one obtains

$$1/\tau_2 = 4k_1M_f + k_{-1}k_{-2}/(k_2 + k_{-2}) \quad \text{(eq 9b of main text)}$$

REFERENCES

Alber, T. (1992) *Curr. Opin. Genet. Dev. 2*, 205−210.

Bernasconi, C. F. (1976) in *Relaxation Kinetics*, Academic Press, New York.

Graddis, T. J., Myszka, D. G., & Chaiken, I. M. (1993) *Biochemistry 32*, 12664−12671.

Harbury, P. B., Zhang, T., Kim, P. S., & Alber, T. (1993) *Science 262*, 1401−1407.

Harbury, P. B., Kim, P. S., & Alber, T. (1994) *Nature 371*, 80−83.

Harrison, S. C. (1991) *Nature 353*, 715−719.

Hodges, R. S., Semchuk, P. D., Taneja, A. K., Kay, C. M., Parker, J. M. R., & Mant, C. T. (1988) *Pept. Res. 1*, 19−30.

Hurst, H. C. (1994) in *Protein Profile* (Sheterline, P., Ed.) pp 123−168, Academic Press, London.

Jackson, S. E., Moracci, M., ElMasry, N., Johnson, C. M., & Fersht, A. R. (1993) *Biochemistry 32*, 11259−11269.

Kaiser, E., Colescott, R. L., Bossinger, C. D., & Cook, P. I. (1970) *Anal. Biochem. 34*, 595−598.

Laue, T. M., Bhairavi, D. S., Ridgeway, T. M., & Pelletier, S. L. (1992) in *Analytical Ultracentrifugation in Biochemistry and Polymer Science* (Harding, S. E., Rowe, A. J., & Horton, J. C., Eds.) pp 90−125, The Royal Society of Chemistry, Cambridge, U.K.

Leder, L., Wendt, H., Schwab, C., Jelesarov, I., Bornhauser, S., Ackermann, F., & Bosshard, H. R. (1994) *Eur. J. Biochem. 219*, 73−81.

Lovejoy, B., Choe, S., Cascio, D., McRorie, D. K., DeGrado, W. F., & Eisenberg, D. (1993) *Science 259*, 1288−1293.

Milla, M. E., & Sauer, R. T. (1994) *Biochemistry 33*, 1125−1133.

Mo, J. M., Holtzer, M. E., & Holtzer, A. (1991) *Proc. Natl. Acad. Sci. U.S.A. 88*, 916−920.

Monera, O. D., Zhou, N. E., Kay, C. M., & Hodges, R. S. (1993) *J. Biol. Chem. 268*, 19218−19227.

Monera, O. D., Kay, C. M., & Hodges, R. S. (1994) *Biochemistry 33*, 3862−3871.

Myszka, D. G., & Chaiken, I. M. (1994) *Biochemistry 33*, 2363−2372.

O'Neil, K. T., & DeGrado, W. F. (1990) *Science 250*, 646−651.

O'Shea, E. K., Rutkowski, R., & Kim, P. S. (1989) *Science 243*, 538−542.

O'Shea, E. K., Klemm, J. D., Kim, P. S., & Alber, T. (1991) *Science 254*, 539−544.

O'Shea, E. K., Rutkowski, R., & Kim, P. S. (1992) *Cell 68*, 699−708.

O'Shea, E. K., Lumb, K. J., & Kim, P. S. (1993) *Curr. Biol. 3*, 658−667.

Ozeki, S., Kato, T., Holtzer, M. E., & Holtzer, A. (1991) *Biopolymers 31*, 957−966.

Pace, C. N. (1986) *Methods Enzymol. 131*, 266−280.

Pace, C. N., Shirley, B. A., & Thomson, J. A. (1989) in *Protein Structure, a Practical Approach* (Creighton, T. E., Ed.) pp 311−330, IRL Press, Oxford.

Patel, L. R., Curran, T., & Kerppola, T. K. (1994) *Proc. Natl. Acad. Sci. U.S.A. 91*, 7360−7364.

Scholtz, J. M., Qian, H., York, E. J., Stewart, J. M., & Baldwin, R. L. (1991) *Biopolymers 31*, 1463−1470.

Wendt, H., Baici, A., & Bosshard, H. R. (1994) *J. Am. Chem. Soc. 116*, 6973−6974.

Zhang, L., & Hermans, J. (1993) *Proteins 16*, 384−392.

Zhou, N. E., Zhu, B.-Y., Kay, C. M., & Hodges, R. S. (1992) *Biopolymers 32*, 419−426.

Zhou, N. E., Kay, C. M., & Hodges, R. S. (1994) *J. Mol. Biol. 237*, 500−512.

Zhu, B.-Y., Zhou, N. E., Semchuk, P. D., Kay, C. M., & Hodges, R. S. (1992) *Int. J. Pept. Protein Res. 40*, 171−179.

BI9426322